IOP Conf. Series: Materials Science and Engineering **274** (2017) 012085 doi:10.1088/1757-899X/274/1/012085

Controllable Growth of Monolayer MoS_2 and $MoSe_2$ Crystals Using Three-temperature-zone Furnace

Binjie Zheng[a], Yuanfu Chen[b]

State Key Laboratory of Electronic Thin Films and Integrated Devices, University of Electronic Science and Technology of China, Chengdu 610054, P. R. China

[a]cloverbibi@vip.qq.com, [b]yfchen@uestc.edu.cn

Abstract. Monolayer molybdenum disulfide (MoS2) and molybdenum diselenide (MoSe2) have attracted a great attention for their exceptional electronic and optoelectronic properties among the two dimensional family. However, controllable synthesis of monolayer crystals with high quality needs to be improved urgently. Here we demonstrate a chemical vapor deposition (CVD) growth of monolayer MoS2 and MoSe2 crystals using three-temperature-zone furnace. Systematical study of the effects of growth pressure, temperature and time on the thickness, morphology and grain size of crystals shows the good controllability. The photoluminescence (PL) characterizations indicate that the as-grown monolayer MoS2 and MoSe2 crystals possess excellent optical qualities with very small full-width-half-maximum (FWHM) of 96 me V and 57 me V, respectively. It is comparable to that of exfoliated monolayers and reveals their high crystal quality. It is promising that our strategy should be applicable for the growth of other transition metal dichalcogenides (TMDs) monolayer crystals.

1. Introduction

The two-dimensional (2D) atomic crystals of transition metal dichalcogenides (TMDs) have attracted tremendous recent interest due to their unique properties and potential applications [1-3]. For instance, at monolayer thickness, the band structures of some TMDs, like MoS_2 and $MoSe_2$, transit from indirect to direct band gap, resulting in dramatic enhancement of photoluminescence [4]. These properties prompt researchers to obtain high-quality monolayer crystals using various approaches, including micromechanical cleavage [5], liquid-phase exfoliation [6], chemical exfoliation [7] and chemical vapor deposition (CVD) [8]. Among them, CVD method is the most promising one to realize high-quality crystals and wafer-scale films. However, most CVD systems used for growing TMD monolayers only include one or two temperature zones. Temperatures of transition metal source, chalcogen source and substrate cannot be controlled independently if their positions are fixed. Moreover, transition metal source, for example moo3 powder, is always put together with substrate in high temperature zone. This brings up an unintended process, MoO_3 powder will react with chalcogen source first and partially be reduced to MoO_2 powder.

To address the issues mentioned above, in this study, we demonstrate a chemical vapor deposition (CVD) growth of monolayer MoS_2 and $MoSe_2$ crystals using three-temperature-zone furnace. The thickness, morphology and grain size of crystals are tunable through control of growth pressure,

temperature and time. Raman and photoluminescence (PL) characterizations are used to confirm the monolayer thickness and high crystal quality. The $MoSe_2$ and MoS_2 monolayer crystals possess an excellent optical quality with very small full-width-half-maximum (FWHM) of 57 me V and 96 me V, which are comparable to that of exfoliated single-crystal monolayers [9]. Most importantly, the principles demonstrated on MoS_2 and $MoSe_2$ can be extended to growth of other TMD crystals or films.

2. Experimental section

2.1. Materials

Molybdenum (VI) oxide (MoO_3, 99.95%), sulfur pieces (S, 99.999%) and selenium powder (Se, 99.999%) were purchased form Alfa Aesar. All materials were used without further purification.

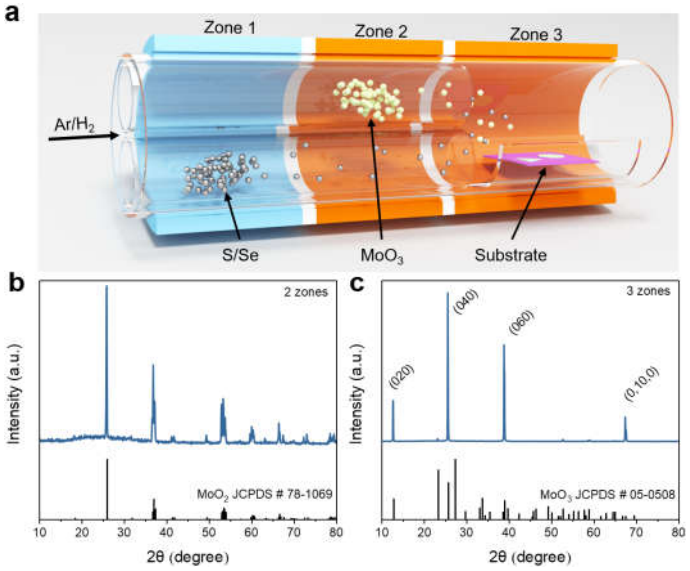

Figure 1. (a) Schematic illustration of growth of monolayer MoS2 or MoSe2 crystals with 3-zones furnace. XRD patterns of MoO3 powders after growth in (b) 2-zones and (c) 3-zones furnaces.

2.2. Growth of monolayer MoS2 crystals

Typically, single crystal silicon substrates with a thermally deposited 300 nm thick silicon oxide (SiO_2/Si) were ultrasonically cleaned with acetone, ethyl alcohol and deionized water for 5 min, respectively. After that, the SiO_2/Si substrates were dried with compressed argon gas immediately, and placed at zone 3 as shown in Figure 1a. Two small quartz tubes respectively loaded with 500 mg of S and 10 mg of MoO_3 powder were put inside the chamber. The MoO_3 powder was located at zone 2 and S located at zone 1. Before heating, the chamber was pumped to 0.5 Pa and refilled with ultrapure argon gas three times to reduce oxygen contamination. Followed the last filling process, argon gas was reduced to 50 sccm as a carrier gas. Then, zone 1, zone 2 and zone 3 were respectively heated to 180 °C, 850 °C and 850 °C at the same time. After growing for 15 min under the atmospheric pressure (1 atm), the heating was stopped, and the furnace was opened immediately to rapidly cool down.

2.3. Growth of monolayer MoSe2 crystals

Typically, like growth of MoS_2 mentioned above, SiO_2/Si substrate, 10 mg of MoO_3 and 500 mg of Se powders were placed at zone 3, zone2 and zone1, respectively. After pumping and refilling process, 50 sccm of argon and 5 sccm of hydrogen gases were introduced as carrier and reaction gases. During the growth, the temperatures of zone 1, zone2 and zone 3 were 340 °C, 850 °C and 750 °C, respectively. When growth was finished, the furnace was cool down rapidly.

2.4. Characterizations

The X-ray diffraction (XRD) patterns were recorded on Rigaku D/MAX-rA diffractometer with Cu Kα radiation. The room temperature Raman and photoluminescence (PL) spectra were recorded by using Horiba LabRAM HR spectrometer with laser wavelength of 532 nm. The optical microscope (OM) photographs were obtained by Olympus BX53 optical microscope.

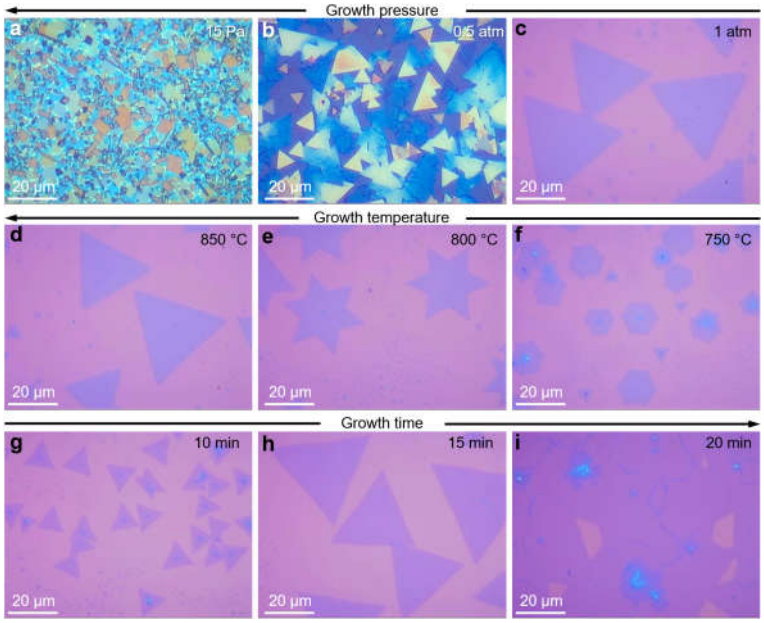

Figure 2. (a) OM images of growth resulted from different growth pressures: (a) 15 Pa, (b) 0.5 atm and (c) 1 ATM; different growth temperatures: (d) 850 °C, (e) 800 °C and (f) 750 °C and different growth time: (g) 10 min, (h) 15 min and (i) 20 min.

3. Results and discussion

As shown in Figure 1a, in 3-zones CVD system with separate small quartz tubes, two kinds of sources evaporate independently without disturbing each other. The XRD patterns in Figure 1b and c demonstrate that the MoO_3 powder is not been reduced by S vapor using 3-zones CVD system compared with 2-zones furnace in which MoO_3 becomes MoO_2. It indicates that 3-zones furnace avoids unintended reaction and the growth process can be more controllable than 2-zones furnace.

Systematically study of the effects of growth pressure, temperature and time on the thickness, shapes and grain size of MoS_2 crystals is shown in Figure 2. Lots of square MoO_2 crystals appear if the growth pressure is ultralow due to the large evaporation of MoO_3. With pressure rising, triangle MoS_2 crystals begin to form, and the thickness decreases [10]. At atmospheric pressure, we get monolayer MoS_2 crystals with size of 50 μm. The morphology of monolayer MoS_2 crystals can be controlled by temperature of growth zone (zone 3). With temperature decreasing, the shape of monolayer MoS_2 crystals change from triangle to hexagram and hexagon due to the temperature dependent migration coefficient of adatoms on substrate [11]. With increasing growth time, the MoS_2 nucleation density decreases and the grain size increases. After 15 min growth, the surface of substrate is covered mainly by large monolayer MoS_2 crystals. Further growth leads to a continuous MoS_2 film resulted from linking together of many nearest-neighbour MoS_2, and MoS_2 crystals start to grown on the film.

To investigate the thickness of MoS_2, we select the sample which is in an intermediate state between crystals and film. Figure 3a clearly shows some connected triangle MoS_2 crystals. Point A is the first layer, AA' stacking with the second layer (point B), and point C is AB stacked with point B [12]. Point D is thick MoS_2 crystals with yellow color. Figure 3b is the optical contrast profile in the

red channel of a color charge-coupled-device (CCD) camera, to estimate the sample thickness [13]. It is noticed that with each additional atomic layer, the contrast decreases by around 10% in few-layer MoS_2 on silicon substrate with a 300-nm oxide layer. The preliminary estimation of the MoS_2 layer number is further verified through Raman spectra shown in Figure 3c and d. The two most dominant peaks located around 382 and 404 cm^{-1} correspond to the in-plane vibration mode (E^1_{2g}) and put-of-plane vibration mode (A_{1g}). As reported earlier [10], the E^1_{2g} peak position has a red shift, while the A_{1g} peak positon has a blue-shift with increasing layer thickness, resulting from the growing influence of interlayer coupling on the electron-phonon processes. Figure 3d shows the thickness-dependent E^1_{2g} and A_{1g} peak frequencies. The differences between E^1_{2g} and A_{1g} for point A, B, C and D are19.5, 12.8, 24.6 and 25.4 cm^{-1}, which is in good agreement with the CVD-grown 1L-, 2L-, 3L- and bulk MoS_2 respectively [14].

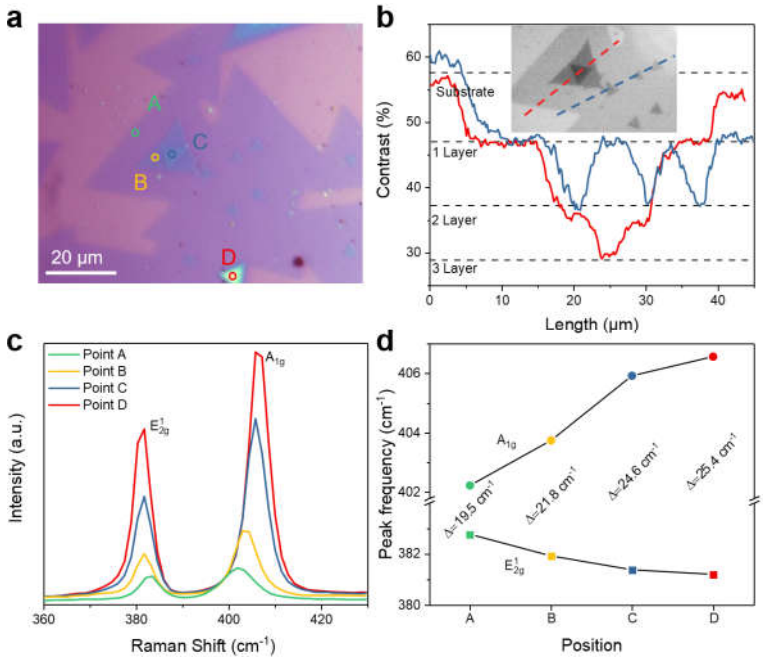

Figure 3. (a) OM photograph of MoS2 crystals. (b) Optical contrast profile in the red channel of the CCD images along the line cuts marked in the inset. (c) Raman spectra from regions marked in (a). (d) The Raman peak frequency of A1g and E12g of MoS2 in (c).

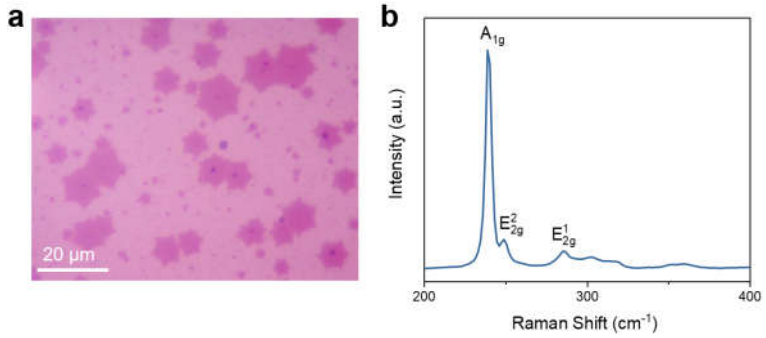

Figure 4. (a) OM photograph and (b) Raman spectrum of monolayer MoSe2 crystals.

To grow monolayer $MoSe_2$ crystals, the temperature of zone 1 was set to 340°C to make sure that the saturated vapor pressure of selenium is same as sulfur. By optimizing the parameters slightly, monolayer $MoSe_2$ crystals were successfully synthesized. Figure 4a shows the hexagon $MoSe_2$ with

average size of 10 μm. Figure 4b shows three characteristic peaks of $MoSe_2$ monolayer: a sharp one at 239.3 cm^{-1} assigned to A_{1g} mode and two broads peaks at 248.9 and 285.6 cm^{-1} assigned to E^2_{2g} shear and E^1_{2g} modes, no B^1_{2g} peak exists [15].

It is well known that monolayer MoS_2 and $MoSe_2$ are direct band gap semiconductors and the quality and thickness of the crystal can be clearly assessed using PL measurements [4]. The blue line in Figure 5 shows one sharp PL peak at 640 and one broad peak at 684 nm, which respectively match the A (1.94 eV) and B (1.81 eV) direct-gap optical transitions of MoS_2 [16]. The red line has a strong peak at 818 nm, corresponding to the direct gap of $MoSe_2$ (1.52 eV) [15]. The FWHM of $MoSe_2$ and MoS_2 are found to be as small as 57 and 96 meV, which is comparable to that of exfoliated monolayers. The excellent optical quality confirms the monolayer thickness of as-grown MoS_2 and $MoSe_2$ and indicates their high crystal quality.

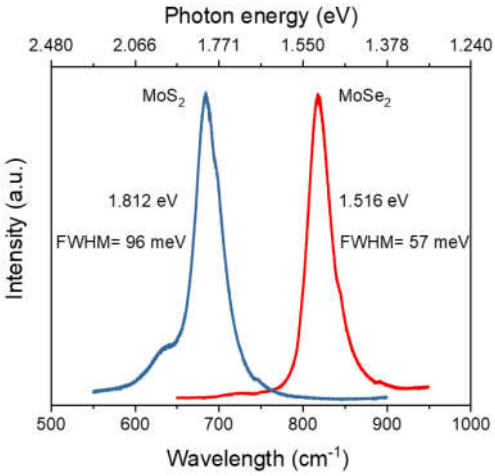

Figure 5. PL spectra of monolayer MoS2 and MoSe2.

4. Conclusion

We demonstrate a CVD growth of monolayer MoS_2 and $MoSe_2$ crystals using three-temperature-zone furnace. The thickness, morphology and grain size of crystals are tunable through control of growth pressure, temperature and time. Raman and PL characterizations confirm the monolayer thickness and high crystal quality. The PL characterizations indicate that the as-grown monolayer MoS_2 and $MoSe_2$ crystals possess excellent optical qualities with very small FWHM of 96 meV and 57 meV, respectively, which are comparable to that of exfoliated monolayers. It is easy to visualize our route might be extended to the growth of other TMDs monolayer crystals.

Acknowledgements

The research was supported by the National Natural Science Foundation of China (51372033), and National High Technology Research and Development Program of China (2015AA034202).

References

[1] Chhowalla M, Liu Z and Zhang H, Chem. Soc. Rev. 44 (2015) 2584-6.
[2] Zheng B, Chen Y, Wang Z, Qi F, Huang Z, Zhang W and Li Y, 2D Mater. 3 (2016) 035024.
[3] Zheng B, Chen Y, Qi F, Wang X, Zhang W, Li Y and Li X, 2D Mater. 4 (2017) 025092.
[4] Zeng H and Cui X, Chem. Soc. Rev. 44 (2015) 2629-42.
[5] Castellanos-Gomez A, van der Zant H S J and Steele G A, 2D Mater. 1 (2014) 011002.
[6] Kim J, Kwon S, Cho D H, Kang B, Kwon H, Kim Y, Park S O, Jung G Y, Shin E, Kim W G, Lee H, Ryu G H, Choi M, Yoon S W, Lee Z and Lee C, Nat. Commun. 6 (2015) 8294.
[7] Peng J, Wu J, Li X, Zhou Y, Yu Z, Guo Y, Wu J, Lin Y, Li Z, Wu X, Wu C and Xie Y, J. Am. Chem. Soc. 139 (2017) 9019-25.

[8] Cain J D, Shi F, Wu J and Dravid V P, ACS Nano 10 (2016) 5440-5.
[9] Tongay S, Zhou J, Ataca C, Lo K, Li J, Grossman J C and Wu J, Nano Lett. 12 (2012) 5576-80
[10] Najmaei S, Liu Z, Zhou W, Zou X, Shi G, Lei S, Yakobson B I, Idrobo J C, Ajayan P M and Lou J, Nat. Mater. 12 (2013) 754-9.
[11] Cui F, Wang C, Li X, Wang G, Liu K, Yang Z, Feng Q, Liang X, Zhang Z, Liu S, Lei Z, Liu Z, Xu H and Zhang J, Adv. Mater. 28 (2016) 5019-24.
[12] Xia M, Li B, Yin K, Capellini G, Ajayan P M and Xie Y H, ACS Nano 9 (2015) 12246-54.
[13] Li L, Kim J, Jin C, Ye G J, Qiu D Y, da Jornada F H, Shi Z, Chen L, Zhang Z, Yang F, Watanabe K, Chen X H, Zhang Y and Wang F, Nat Nanotechnol 12 (2017) 21-5.
[14] Zhang X, Qiao X F, Wu J B, Jiang D S and Tan P H, Chem. Soc. Rev. 44 (2015) 2757-85.
[15] Gong Y, Ye G, Lei S, Shi G, He Y, Lin J, Zhang X, Vajtai R, Pantelides S T, Zhou W, Li B and Ajayan P M, Adv. Funct. Mater. 26 (2016) 2009-15.
[16] van der Zande A M, Huang P Y, Chenet D A, Berkelbach T C, You Y, Lee G H, Heinz T F, Reichman D R, Muller D A and Hone J C, Nat. Mater. 12 (2013) 554-61.